

Investigation of shear band strengthening by using different strengthening criteria

Elnaz Hadjiloo, Jürgen Grabe²

^{1,2}Technische Universität Hamburg, Institut für Geotechnik und Baubetrieb, Harburger Schloßstraße 36, 21073 Hamburg, Germany

#Corresponding author: elnaz.hadjiloo@tuhh.de

ABSTRACT

To prevent a critical failure mechanism, it is possible to simply strengthen the potential shear bands, which is a patented idea. The localization of potential shear bands that are most likely to form shear can be calculated. Before these shear bands can appear, they can be strengthened by injecting a cement suspension or using jet grouting at the locations where the most likely shear bands would occur. As a result, it is possible to increase the bearing capacity of the geotechnical system by focusing solely on the shear bands that are most likely to form, minimizing the use of materials. Numerical modeling is employed to analyze the increase in bearing capacity. Four criteria for strengthening the shear bands are applied by incorporating them into a hypoplastic soil model, taking into consideration the material transition from soil to cement, as well as intermediate materials that can arise from jet grouting, which are mixtures of soil and cement. Two fundamental geotechnical systems, namely a shallow foundation and a retaining wall, are analyzed using ABAQUS/Standard for finite element analysis. The results demonstrate the potential of numerical modeling to identify the most critical localized areas in the soil that require strengthening, as well as the substantial increase in bearing capacity achieved after reinforcing the identified areas.

Keywords: Shear band enhancement; soil improvement; increase of bearing capacity.

1. Introduction

In practice, the typical approach to increasing the bearing loads of geotechnical constructions involves the use of structural elements designed to intersect the forming shear zone. These elements include poles, micropiles, anchors, soil nails, and geotextiles. Another method used to enhance the shear strength of the soil is the incorporation of chemical additives. For instance, nanoparticles have been studied for their potential to increase soil shear strength, although they are not commonly employed in practical applications. Experimental studies conducted by (Sadrjamali et al. 2015) revealed that the use of nanoparticles can actually reduce shear strength due to the large specific surface area of the nanoparticles, resulting in unstable nano-silica compounds in the soil. Initially, there may be a temporary increase in shear strength, followed by a subsequent decrease. Consequently, the chemical method of employing nanoparticles is not considered suitable for enhancing soil shear strength.

In the present project, a different approach known as shear band strengthening is utilized. This method focuses on modifying the mechanical properties of the soil within the forming shear zones and their vicinity. The concept of shear band strengthening was developed and patented by the Technical University of Hamburg (Grabe & Pucker, 2012). Under the influence of external loads, thin shear zones or shear joints form within the soil. The position and shear strength of these zones significantly impact the load-bearing capacity of geotechnical structures. Shear zones are well-known to be the weakest

zones under a geotechnical structure and are susceptible to failure.

The method employed in this project involves identifying and calculating the most likely shear band to form. These are the shear bands that would occur under the lowest external load compared to other potential shear bands. These identified shear bands are then reinforced by locally injecting cement. As a result, the most probable shear bands are prevented from forming, and instead, other shear bands with higher bearing capacities are formed. In the case of retaining walls, this means that a shear band with a greater sliding surface angle needs to form, resulting in reduced active earth pressure on the retaining wall. The principle is visually depicted in Figure 1.

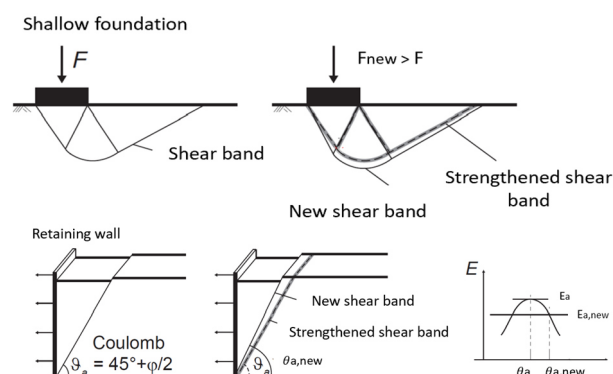


Figure 1. Principle of new shear band formation after strengthening of most likely shear band for a shallow foundation (above) and a retaining wall (below).

2. Methodology

2.1. Previous work

The concept of strengthening potential shear bands beneath or adjacent to a geotechnical construction was subjected to experimental investigation by (Seitz 2021). Additionally, numerical analysis of this method has been conducted using the commercial software OptumG2, employing a soil model based on Mohr-Coulomb principles (Seitz 2021). The findings from both the experimental and numerical investigations carried out by (Seitz 2021) demonstrate the potential for enhancing the bearing capacity of geotechnical structures.

2.2. Current work

In this paper, the authors build upon the previous work conducted by (Seitz 2021). However, they introduce a novel approach by shifting the numerical investigations from the Finite Element Limit Analysis (FELA) method using the commercial software OptumG2 to the Finite Element Method (FEM) with the utilization of the commercial software ABAQUS/Standard. This allows for the incorporation of higher-order soil models in the numerical investigations. Specifically, a hypoplastic soil model based on (Niemunis 2003) is employed, considering a material transition from soil to mortar as proposed by (Pucker 2013). The hypoplastic soil model enables the representation of both soil and mortar by utilizing an interpolation factor ranging between 0 and 1 to facilitate the transition from soil to mortar. To govern the transition from soil to mortar, the authors of this paper have incorporated various strengthening criteria. These criteria determine the conditions under which the switch from soil to mortar should occur. The specifics of these criteria are elaborated upon in the subsequent subsection.

2.2.1. Strengthening criteria

In the soil model, four distinct strengthening criteria have been selected and incorporated as the strengthening function, denoted as k . Out of these criteria, two are stress-based, one is strain-based, and one is based on physical work.

Shear dissipation

As one strengthening criterion, the shear dissipation is chosen which is a criterion based on the physical work. It is defined as the scalar product of the deviatoric stress tensor \mathbf{s} and the deviatoric distortion tensor \mathbf{e} , as shown in Equation (1). The strengthening function is denoted as $k(D_s)$ and is represented by a parabolic function, as depicted in Figure 2. Equation (2) defines the function $k(D_s)$ as the ratio of the current squared value of the shear dissipation D_s^2 to the maximum squared shear dissipation $D_{s,max}^2$. The decision to use a parabolic function is based on investigations into the convergence behaviour of different function types.

$$D_s = \mathbf{s} : \mathbf{e} = s_{ij} e_{ij} \quad (1)$$

$$k(D_s) = \frac{D_s^2}{D_{s,max}^2} \quad (2)$$

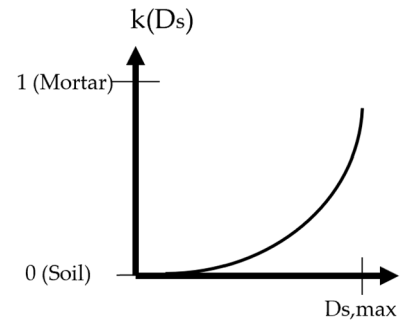


Figure 2. Strengthening function $k(D_s)$.

Degree of nonlinearity

As the second strengthening criterion, the degree of nonlinearity Y is utilized, which is a stress-based criterion. The degree of nonlinearity indicates the proximity of a stress state to the limit state, as defined by (Matsuoka and Nakai 1985). Y is a component of the hypoplasticity soil model employed and depends on the stress invariants I_1, I_2 and I_3 as defined in Equation (3). The stress invariants I_1 and I_2 are defined based on the trace of the stress tensor, while the stress invariant I_3 is defined as the determinant of the stress tensor, as shown in Equations (4), (5) and (6). The strengthening function $k(Y)$ is defined in Equation (7) as the ratio of the current value of the degree of nonlinearity Y to the maximum value of the degree of nonlinearity Y_{max} . In this case, a linear strengthening function is chosen for $k(Y)$, as illustrated in Figure 3.

$$Y = \frac{\frac{I_1 I_2}{I_3} - 9}{\frac{9 - \sin^2(\varphi)}{1 - \sin^2(\varphi)} - 9} \quad (3)$$

$$I_1 = \text{tr}(\boldsymbol{\sigma}) \quad (4)$$

$$I_2 = \frac{1}{2} [\text{tr}(\boldsymbol{\sigma})^2 - \text{tr}(\boldsymbol{\sigma}^2)] \quad (5)$$

$$I_3 = \det(\boldsymbol{\sigma}) \quad (6)$$

$$k(Y) = \frac{Y}{Y_{max}} \quad (7)$$

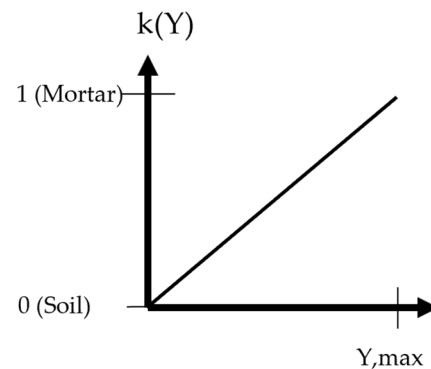


Figure 3. Strengthening function $k(Y)$.

Shear strain

As a strain-based criterion, the shear strain ε_{12} is chosen, as indicated in Equation (8). A parabolic strengthening function is employed for the function $k(\varepsilon_{12})$, as shown in Figure 4. The function is defined as the ratio of the current squared value of the shear strain ε_{12}^2 to the maximum squared shear strain $\varepsilon_{12,max}^2$, as depicted in Equation (9).

$$\varepsilon_{12} = \frac{1}{2} \left(\frac{\partial u_i}{\partial x_j} + \frac{\partial u_j}{\partial x_i} \right) \quad (8)$$

$$k(\varepsilon_{12}) = \frac{\varepsilon_{12}^2}{\varepsilon_{12,max}^2} \quad (9)$$

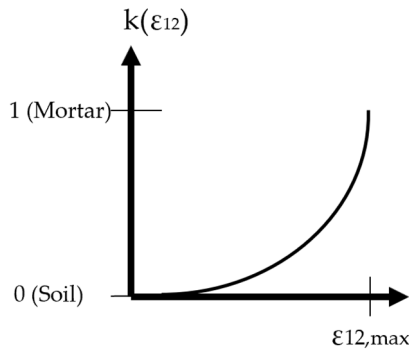


Figure 4. Strengthening function $k(\varepsilon_{12})$.

Mobilized friction angle

The fourth criterion, which is also stress-based, is the mobilized friction angle φ_{mob} , as shown in Equation (10). The mobilized friction angle is defined based on the principal stresses σ_1 and σ_3 , according to Equations (11) and (12). The corresponding strengthening function $k(\varphi_{mob})$ is defined in Equation (13) as the ratio of the mobilized friction angle to the maximum friction angle φ_{max} , as specified in Equation (13). A linear strengthening function is chosen for $k(\varphi_{mob})$, as illustrated in Figure 5.

$$\varphi_{mob} = \arcsin \left(\frac{\sigma_1 - \sigma_3}{\sigma_1 + \sigma_3} \right) \quad (10)$$

$$\sigma_1 = \max(\sigma_1, \sigma_2, \sigma_3) \quad (11)$$

$$\sigma_3 = \min(\sigma_1, \sigma_2, \sigma_3) \quad (12)$$

$$k(\varphi_{mob}) = \frac{\arcsin \left(\frac{\sigma_1 - \sigma_3}{\sigma_1 + \sigma_3} \right)}{\varphi_{max}} \quad (13)$$

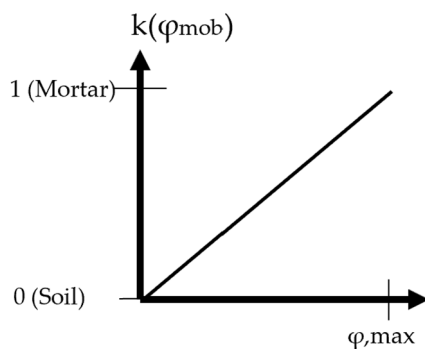


Figure 5. Strengthening function $k(\varphi_{mob})$.

When utilizing the criteria based on shear dissipation, degree of nonlinearity, or shear strain, it is necessary to determine the maximum possible values of these criteria, denoted as $D_{s,max}$, Y_{max} and $\varepsilon_{12,max}$, respectively, while deactivating the strengthening functions. This can be achieved by utilizing solution-dependent state variables (SDVs) in ABAQUS. In a subsequent calculation, the chosen strengthening function is activated, and the maximum value obtained from the same boundary value problems (with identical loads and boundary conditions, etc.) is considered. In the case of the mobilized friction angle, the maximum friction angle can be selected as the critical angle, which is also defined as a property value in ABAQUS when using the soil model as a user routine. A sudden transition from natural soil to strengthened soil (mortar) is not employed, as the non-steady transition during equilibrium iteration is crucial.

The reason for implementing different strengthening criteria is to allow the user to compare the results obtained from various criteria for a given boundary value problem and determine which criterion provides a better fit. Different criteria are chosen for this comparison, including two stress-based criteria, one strain-based criterion, and one work-based criterion. All selected criteria have the potential to describe critical areas within the soil, where shear bands or shear zones are formed. The implementation of these criteria is described in the following subsection.

2.2.2. Implementation of the strengthening criteria

Two different approaches are chosen for the implementation of the strengthening criteria. The first approach involves directly implementing the aforementioned criteria within the user routine (soil model) used in ABAQUS. This allows for internal strengthening within ABAQUS. The second approach involves controlling the strengthening process by utilizing the same criteria and implementing them in the commercial software MATLAB. MATLAB is then used to call ABAQUS software. In this case, the strengthening occurs externally and not within the user routine itself.

Internal implementation

The internal implementation involves directly adding the mentioned strengthening functions into the user routine UMAT, which is part of the used soil model. These functions are incorporated into the existing soil model. The interpolation factor, which determines the proportion of natural soil or strengthened soil (mortar) present, is defined within the user routine and controlled by the implemented functions. Communication between the user routine and ABAQUS occurs through the variable *temp*, which is passed from ABAQUS to the user routine for each increment. This variable *temp* corresponds to the interpolation factor *k*. The implemented strengthening functions are defined in the user routine based on the value of *temp*. As a result, the state of strengthening is updated in each increment and communicated between the user routine and ABAQUS. The criteria have been implemented in such a way that the strengthening only occurs during the loading phase and not during the calculation of the initial stress state.

Figure 6 illustrated the transtion from soil (corresponding to state 0) to strengthened soil (corresponding to state 1).

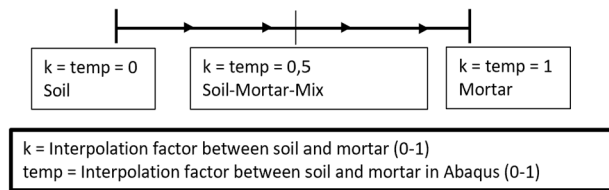


Figure 6. Transition from soil to strengthened soil (mortar).

External implementation

The external implementation can be described through the following steps:

1. Calculation of the boundary value problem in ABAQUS to initialize the initial stress state.
2. Calculation of the boundary value problem while considering the calculated initial stresses. During this calculation, the strengthening function is deactivated, resulting in a value of $k = 0$.
3. The results from the previous step are saved as an .odb file.
4. Using Python scripting, the relevant values of the employed strengthening criterion (e.g. D_s , Y , ε_{12} or φ_{mob}) are extracted as solution-dependent variables.
5. The extracted values are filtered by using a defined threshold value. The maximum value is determined, and it is checked at which nodes the defined percentage of the maximum value (threshold value) is reached. Nodes that meet the threshold value are set to $k = temp = 1$, indicating strengthened soil. The remaining nodes are set to $k = temp = 0$ using a Heaviside filter. The maximum value is automatically updated at each calculation step, ensuring adaptive adaptation.
6. The resulting list of material points with assigned values of 0 or 1 is written into a new input file called temp.inp using MATLAB.
7. The calculation from step 2 is performed again, this time considering the interpolation parameters from step 6 (temp.inp). Consequently, the strengthened material points are taken into account in this step.

The mentioned steps of the external implementation are summarized in the flowchart shown in Figure 7.

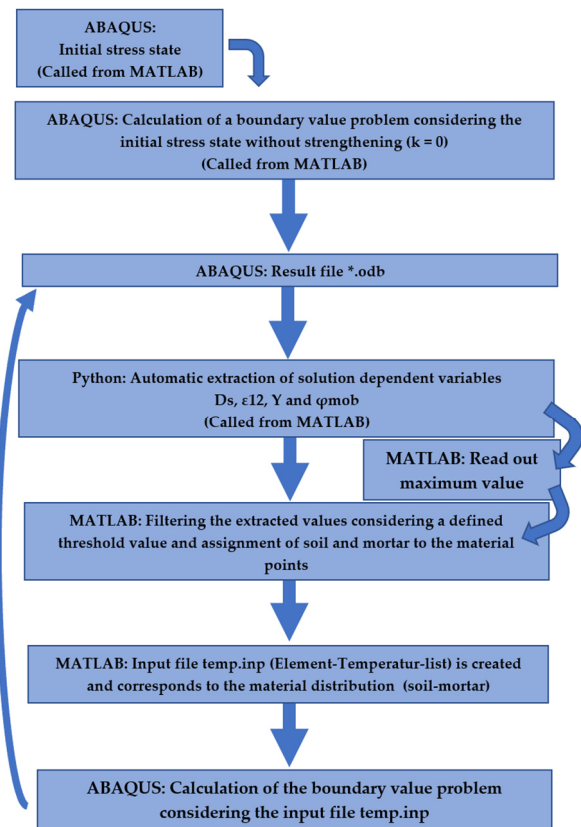


Figure 7. Flowchart for the external implementation of the strengthening criteria.

The advantage of the external implementation using MATLAB is that the user has control over the number of iterations to be performed. This allows for an iterative process where each iteration considers the previously strengthened system and incorporates new strengthened areas based on the external load. To avoid situations where previously strengthened zones are reverted to soil due to their apparent lack of criticality resulting from mortar injection, a holding criterion is introduced. This criterion prevents strengthened areas from being changed back to unstrengthened areas. This holding criterion is implemented both in the internal implementation within the user routine and in the external implementation within MATLAB. By incorporating this restriction, the risk of inadvertently reversing the strengthening process is mitigated.

3. Numerical investigation

In the subsequent subsections, the numerical models investigated and their corresponding results are presented and discussed.

3.1. Numerical models

Two numerical models were investigated in this study. The first model is a strip foundation, as depicted in Figure 8. The strip foundation is represented as a rigid foundation in the numerical analysis. The second model is a retaining wall, specifically considering the case of active earth pressure. The wall is horizontally displaced in parallel to prevent any zone break, taking into account the findings from experimental investigations conducted

by (Seitz 2021). Figure 9 illustrates the configuration of the retaining wall in the numerical model.

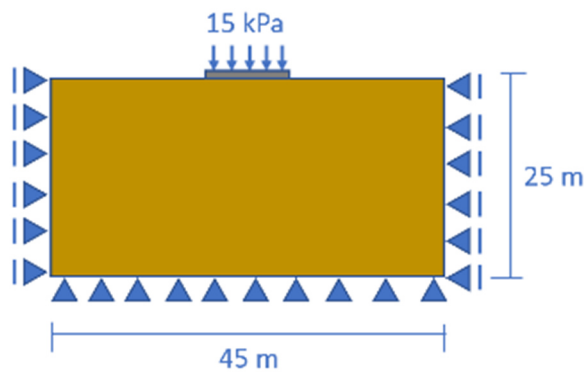


Figure 8. Numerical model: strip foundation.

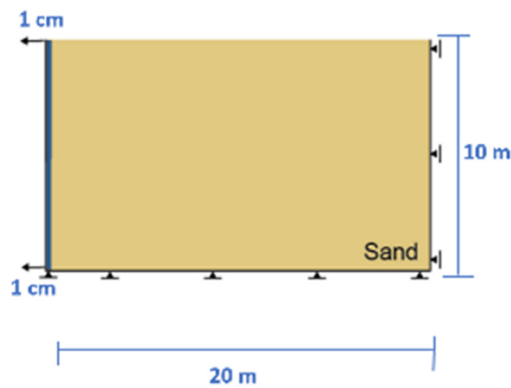


Figure 9. Numerical model: retaining wall.

3.2. Results

Strip foundation

The strip foundation was examined using all four strengthening criteria. The results of the calculations are presented as the values of the strengthening function, k . This distribution represents the distribution of the strengthened soil (mortar) and the natural (unstrengthened) soil, as illustrated in Figure 10. In Figure 10, the red zones indicate areas where 100 % strengthening has been achieved based on the employed strengthening criterion. The yellow, orange, and green zones represent mixed zones of natural and strengthened soil, resulting from the gradual transition from natural to strengthened soil ($0 < k < 1$). It can be observed that, as expected, the shear zones typically initiate below the corners of the strip foundation in almost all four cases. However, the results based on the $k(Y)$ criterion do not exhibit as distinct shear zones as those obtained from the other strengthening functions in the case of a rigid strip foundation. Interestingly, when considering a constant distributed line load instead of a rigid foundation, the results based on the $k(Y)$ criterion demonstrate a clear tendency of a hardened shear zone initiation, as depicted in Figure 11. This indicates that the initiation of shear zones can be detected and strengthened using all implemented strengthening criteria.

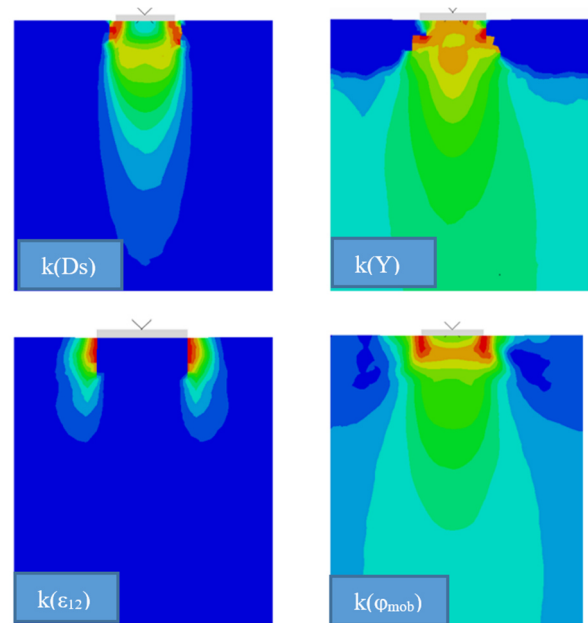


Figure 10. Numerical results of the investigated strip foundations (rigid) with different strengthening criteria: material distribution of strengthened and natural soil (red = strengthened zones, dark blue = natural soil, rest = soil-mortar mixed zones); internal implementation.

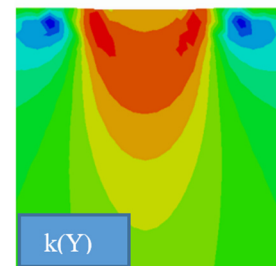


Figure 11. Numerical results of the investigated strip foundations (not rigid) with different strengthening criterion $k(Y)$: material distribution of strengthened and natural soil (red = strengthened zones, green = natural soil, rest = soil-mortar mixed zones); internal implementation.

The convergence behavior and calculation time of the employed criteria exhibit differences due to the updating of criterion-relevant quantities in each iteration step of the implicit calculation. As these quantities simultaneously influence the material change, it affects the convergence behavior and calculation time. The previously presented results were obtained using the internal implementation. In the external implementation, it is possible to control the number of calculation runs in MATLAB. The results obtained from the external implementation align with expectations and match the results of the internal implementation for the first calculation run. In the second calculation run, the strip foundation is subjected to loading and strengthening based on the results of the first calculation run. The results after the second calculation run are depicted in Figure 12. These results are unfiltered, showing mixed zones of both strengthened and unstrengthened areas in the soil. For all criteria except $k(\epsilon_{12})$, the initial shear zone continues to evolve in accordance with the active Rankine zone. However, the initially strengthened area of the shear zone from the first calculation run is no longer strengthened in the second calculation run (indicated by

black circles). This occurs because in the second calculation run, the initial shear zone area is considered to be non-critical due to the strengthening implemented in the previous calculation run. An exception to this behavior is observed in the criterion based on $k(\varepsilon_{12})$.

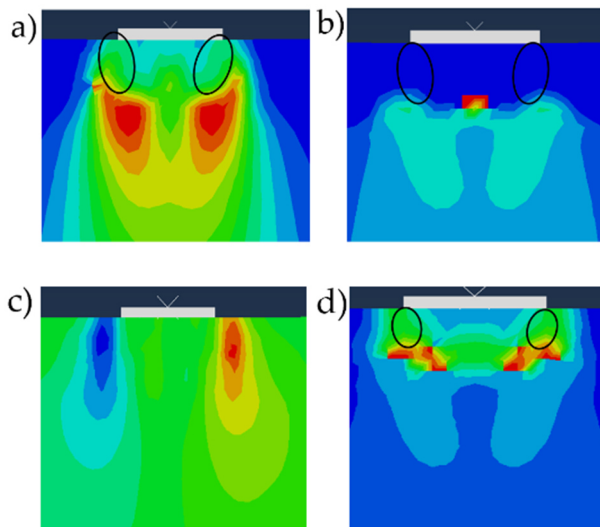


Figure 12. Numerical results of the investigated strip foundations with $k(Ds)$ (a), $k(Y)$ (b), $k(\varepsilon_{12})$ (c) and $k(\phi_{mob})$ (d): material distribution of strengthened and natural soil; external implementation.

The quantitative results after one calculation run are presented in Figure 13. The results illustrate the impact of strengthening based on the criterion $k(Ds)$. The figures depict both the mid-point of the strip foundation and the corner areas. The findings indicate that strengthening the corner areas significantly increases the vertical force required to achieve the same settlement. For instance, in the absence of strengthening, a settlement of 0.6 cm corresponds to a vertical force of approximately 12 kN/m. In the middle of the foundation, the strengthening has a minor effect on the corresponding vertical force for the same vertical displacement. In fact, the strengthening reduces the vertical force for the same displacement when compared to the case without strengthening. This observation can be attributed to force redistribution resulting from the strengthening at the corners.

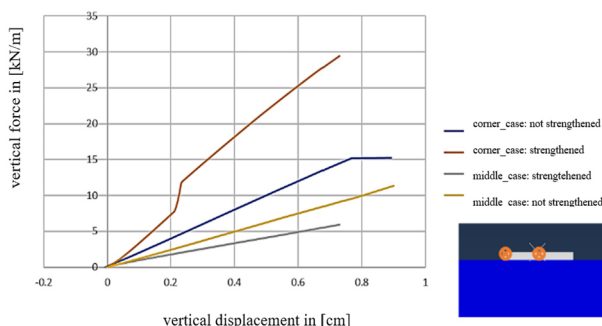


Figure 13. Force displacement curve for the not strengthened and strengthened case based on criterion $k(Ds)$.

Retaining wall

Figure 14 depicts the outcomes of the analysis conducted on the retaining wall using the aforementioned. It is evident that, in general, a shear zone

is observed at the anticipated position, commencing from the base of the retaining wall. The straight black lines highlighted in Figure 14 provide clarification regarding the orientation of the shear zone. When employing the criterion $k(\phi_{mob})$, the shear zone diffuses and does not exhibit a distinct inclination towards the upper edge, unlike the other criteria.

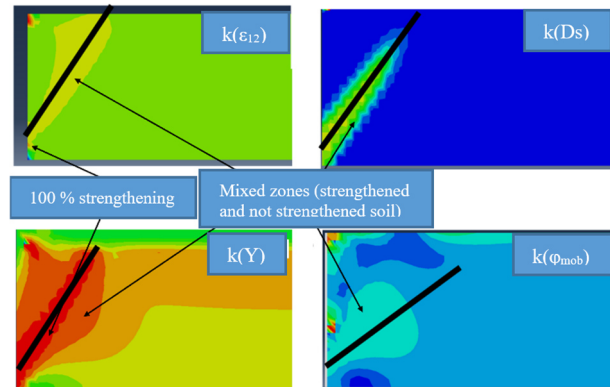


Figure 14. Numerical results for a retaining wall (case: active earth pressure) with different strengthening criteria: material distribution of strengthened and natural soil; internal implementation.

The results from the external implementation align closely with those obtained from the internal implementation during the initial calculation run. Figure 15 provides an example of the outcomes from a second calculation run conducted using an external implementation, employing the strengthening function $k(Y)$. The left side displays the results from the first calculation run, while the right side presents the results from the second calculation run. It is apparent that, similar to the case of the strip foundation, the section of the shear zone that was reinforced in the first calculation run is no longer strengthened in the second run. Consequently, the shear zone in the second run does not directly continue from the beginning of the shear zone. The initial section of the shear zone, which was considered a critical region in the first run, has transformed into natural soil in the second run. The results indicate that the angle of the sliding surface is approximately 55° after the first calculation run and subsequent strengthening. However, in the second run, the angle increases to around 60° . This higher angle diminishes the area of the active earth pressure wedge that acts on the retaining wall, thereby reducing its impact.

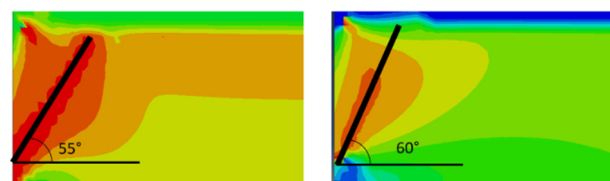


Figure 15. Numerical results for a retaining wall for a second calculation run (case: active earth pressure) with the strengthening criterion $k(Y)$ (not filtered): material distribution of strengthened and natural soil (first run: left; second run: right) external implementation.

3.3. Discussion

The results indicate that all implemented criteria are effective in detecting and strengthening shear bands. However, their applicability is subject to certain restrictions, primarily dependent on the specific boundary value problem under investigation and the chosen mesh size. Therefore, it is not possible to make a generalization regarding the suitability of these criteria. For instance, the criterion $k(Y)$ appears to be more suitable for non-rigid foundations. This may be due to convergence issues arising from the interaction between the foundation and the soil, as both the material distribution update and the hypoplastic soil model rely on the degree of nonlinearity. Furthermore, the results demonstrate that both internal and external implementations are capable of identifying and strengthening shear zones. The main distinction between these two approaches lies in the timing of material distribution updates. In the internal implementation, the update occurs simultaneously in each increment, whereas in the external implementation, it is conducted after completing one full calculation run. The advantage of using an external implementation is that MATLAB can automatically determine the number of calculation runs in ABAQUS based on the results of each previous calculation. Additionally, the findings indicate that strengthening the beginning of potential shear bands is sufficient. Strengthening only the initial section yields positive effects on the force-displacement curve and the resulting active earth pressure on the wall. This observation aligns with experimental observation by (Seitz 2021) and supports the comparison of corresponding forces for the same vertical displacement with and without strengthening, as demonstrated by (Pucker & Grabe 2010). In the case of the strip foundation, the most significant effects of shear band strengthening are observed at the corners of the foundation where the strengthening is applied. In the middle of the foundation, the results indicate force redistribution effects. To address the transition of formerly strengthened zones to areas without strengthening in the second calculation run, an additional retention criterion can be implemented. In the external implementation using ABAQUS, this can be achieved by modifying the resulting temperature-node list from the second calculation run onwards to include the nodes requiring strengthening from the first calculation run. In ABAQUS internal implementation, a similar retention criterion is implemented in the user routine (UMAT), ensuring that the points strengthened in the previous calculation step maintain a strengthening degree of 100 % in subsequent calculation steps. This approach necessitates defining different load steps within a single calculation run in ABAQUS.

4. Conclusions

In conclusion, the study demonstrated the feasibility of automatically detecting and strengthening potential shear bands through the utilization of a higher order soil and an automated calculation process. The results highlight significant potential for cost and material

savings in both strip foundation and retaining wall designs. Strengthening the potential shear bands enhances the bearing capacity, enabling the structures to achieve higher load-bearing capabilities with reduced material usage. The identified potential for material is particularly noteworthy, as it contributes to reducing both emissions and costs associated with construction projects. By optimizing the strengthening strategies and employing automatic detection methods, further improvements can be achieved in terms of cost-effectiveness and environmental sustainability. Future research in this field will focus on refining the retention criteria used in the analysis. The aim is to optimize and tailor the strengthening strategies based on the specific characteristics of each problem, thereby enhancing the overall performance of the structures. Additionally, future work will concentrate on enhancing the contact algorithm between the natural and strengthened soil. The objective is to develop a more realistic contact model that reduces the dependence on mesh size, resulting in more general and versatile models. This advancement would contribute to a more accurate representation of the soil-structure interaction and enhance the overall reliability and applicability of the analysis. In summary, the study demonstrated the potential benefits of automated detection and strengthening of shear bands, paving the way for more efficient and sustainable geotechnical design practices.

Acknowledgements

The authors are grateful for the financial support provided by funding agency DFG (Deutsche Forschungsgesellschaft).

References

- Matsuoka, H., Nakai, T. 1985. "Relationship Among Tresca, Mises, Mohr-Coulomb And Matsuoka-Nakai failure criterion." *Soils and Foundations* 25, no. 4 (December): 123-128. https://doi.org/10.3208/sandf1972.25.4_123
- Niemunis, A. 2003. "Extended Hypoplastic Models for Soil." Habilitation, Ruhr-Universität Bochum, Publication of Institut für Grundbau und Bodenmechanik, Heft 34.
- Pucker, T. 2013. "Stoffmodell zur Modellierung von stetigen Materialübergängen im Rahmen der Optimierung geotechnischer Strukturen." Dissertation, Technische Universität Hamburg. Publication of Institut für Geotechnik und Baubetrieb. Heft 28.
- Pucker, T., Grabe, J. 2010. "Traglasterrhöhung von Fundamenten durch gezielte Bodenverbesserung." *Baugrundverbesserung in der Geotechnik*. Siegen, Deutschland: 261-275.
- Sadrjamali, M., Athar, S., Negahdar, A. 2015. "Modifying Soil Shear Strength Parameters Using Additives in Laboratory Condition." *Current World Environment* 10, no. 1 (May): 120-130. <http://dx.doi.org/10.12944/CWE.10.Special-Issue1.17>
- Seitz, K.-F. 2021. "Zur Topologieoptimierung von geotechnischen Strukturen und zur Tragfähigkeitssteigerung des Baugrunds durch Scherfugenverfestigung." Dissertation, Technische Universität Hamburg. Publication of Institut für Geotechnik und Baubetrieb. Heft 45.